

Optimal Solvent Design for Extractive Distillation Processes: A Multi-objective Optimization based Hierarchical Framework

Teng Zhou^{1,*}, Zhen Song¹, Xiang Zhang², Rafiqul Gani³, Kai Sundmacher^{1,4}

¹ *Process Systems Engineering, Max Planck Institute for Dynamics of Complex Technical Systems,
Sandtorstr. 1, D-39106 Magdeburg, Germany*

² *Department of Chemical and Biological Engineering, The Hong Kong University of Science and
Technology, Clear Water Bay, Hong Kong, China*

³ *PSE for SPEED, Skyttemosen 6, DK 3450 Allerød, Denmark*

⁴ *Process Systems Engineering, Otto-von-Guericke University Magdeburg, Universitätsplatz 2, D-39106
Magdeburg, Germany*

* Corresponding author: zhout@mpi-magdeburg.mpg.de (Teng Zhou)

Abstract

Extractive distillation is a widely accepted and commercialized process for separating azeotropic mixtures compared to conventional distillation. The search for high-performing solvents, or entrainers, needed in extractive distillation is a challenging task. The heuristic guideline or experiment based method for the screening of entrainers is usually not very efficient and limited to the existing, well-known solvents. In this contribution, we propose a multi-stage theoretical framework to design solvents for extractive distillation. A multiobjective optimization based computer-aided molecular design (MOO-CAMD) method is developed and used to find a list of Pareto-optimal solvents. In the MOO-CAMD method, two important solvent properties (i.e., selectivity and capacity) that determine the extractive distillation efficiency are simultaneously optimized. The next step involves a further screening of the Pareto-optimal solvents by performing rigorous thermodynamic calculation and analysis. Finally, for each of the remaining solvents, the extractive distillation process is optimally designed and the best candidate showing the highest process performance is ultimately identified. The overall design framework is illustrated through an example of the n-hexane and methanol separation.

Introduction

Distillation is perhaps the most important separation technique in the chemical and petrochemical industries and thus the optimal design of distillation processes can greatly influence the profitability of a plant. The operation of distillation columns is based on the varying volatilities of the components targeted for separation. However, sometimes the relative volatility is close to unity or azeotropes exist and conventional distillation is unable to achieve the desired separation. The primary methods used industrially for the separation of close-boiling and azeotropic mixtures are heterogeneous azeotropic distillation and homogeneous extractive distillation, otherwise known simply as extractive distillation. Compared to the heterogeneous azeotropic distillation, extractive distillation is generally more energy efficient, which is especially true when heat integration is considered.¹ In extractive distillation, a suitable separating solvent, the entrainer, is added to the original mixture in order to increase the relative volatility of the compounds which consequently promotes the separation. Thus, the selection of the entrainer can have a deciding effect on the performance of an extractive distillation process.

Two primary methods for solvent selection exist. One is the so-called “experience-and-experiment”, where solvent candidates are initially selected based on experience or by using heuristics.^{2,3} Afterwards, phase equilibrium experiments or residue curve map (RCM) calculations are performed for each of the selected solvents. Based on the results, the best performing solvent can be identified. Despite its ease of application, this method is limited by its reliance on experience and that it can be time-consuming. The method is therefore limited to the well-known separation systems and a relatively small number of existing solvents. The other approach takes advantage of modern molecular property models, numerical algorithms, and computing power that have enabled the development and use of computer-aided molecular

design (CAMD) methods. CAMD, introduced by Gani and Brignole⁴, is a blanket term for the use of computational based strategies in the rational selection or design of molecules that possess known, desirable properties based on a given set of molecular building groups. CAMD approaches have been broadly implemented for designing solvents used in reactions⁵⁻¹³ and for separations¹⁴⁻²⁴.

In general, CAMD problems are formulated and solved as optimization problems where the groups used to build the molecule are left as optimization variables. For CAMD-based separation solvent design, two important solvent thermodynamic properties, i.e., selectivity and capacity (see the next section for the definition), are usually posed as the objective function with solvent physical properties such as boiling point written as constraints. Lek-utaiwan et al.²⁵ used the ICAS ProCAMD software²⁶ where CAMD methods are implemented to find suitable entrainers for extractive distillation processes. The properties considered include separation selectivity, melting and boiling temperatures. Kossack et al.²⁷ optimized the selectivity while designing solvents for the separation of acetone and methanol. They found that using the selectivity as the single objective is not a satisfactory solvent selection criterion. They recommended to use the product of selectivity and capacity as the CAMD objective function. Chen et al.²⁸ and Lei et al.²⁹ set lower bounds for both selectivity and capacity in their CAMD program to design entrainers for hydrocarbon separation using extractive distillation. Despite the consideration of both criteria, the effect of solvents on the process performance has not been investigated. It is clear that the process operating conditions can influence the solvent selection. Not only that, but the selected solvent also determines the optimal operating conditions of the process. The best way to capture this interaction is to perform integrated solvent and process design. However, considering the

difficulty in solving these integrated design problems to global optimum, solvent and process design are usually performed sequentially.³⁰⁻³⁵

In this work, we propose a multi-objective optimization based CAMD method to design solvents for extractive distillation processes, which efficiently captures the tradeoff between solvent selectivity and capacity. The resulting solvents are further screened via the prediction and analysis of RCMs. For each of the remaining solvents, the extractive distillation process is optimally designed and the best solvent showing the highest process performance is finally identified. This multi-step design framework is illustrated with a selected example of the n-hexane and methanol separation where the simple distillation is not applicable due to the existence of azeotrope. The results obtained in each step will be presented and discussed separately in the following sections.

Thermodynamic fundamentals

When using extractive distillation to separate a two-component mixture, a suitable solvent is added to increase the relative volatility of the two components. It then becomes possible to separate the mixture with one pure component as the distillate and the other removed together with the solvent in the bottoms. The second component can then be easily separated from the high boiling solvent in a second distillation column. The relative volatility of the components *A* and *B* with an ideal vapor phase is defined by

$$\alpha_{AB} = \frac{y_A/x_A}{y_B/x_B} = \frac{\gamma_A P_A^{sat}}{\gamma_B P_B^{sat}} \quad (1)$$

y and x are the molar fractions in the vapor and liquid phases, respectively. γ is the activity coefficient. P^{sat} is the saturated vapor pressure. Since the vapor pressure ratio remains constant at a given temperature, solvent influences the relative volatility only by changing γ_A/γ_B . This ratio is called solvent (separation) selectivity, S_{AB} .

$$S_{AB} = \frac{\gamma_A}{\gamma_B} \quad (2)$$

If one were to conduct a rigorous comparison of solvents, this would require determining their respective selectivities at a consistent solvent composition. However, the selectivity usually increases linearly with the solvent concentration. Thus, predicting the selectivity at the infinite dilution condition provides a reasonable estimation of the solvent's overall selectivity.

$$S_{AB}^{\infty} = \frac{\gamma_A^{\infty}}{\gamma_B^{\infty}} \quad (3)$$

Another important measure to assess the potential of a solvent as the extractive distillation entrainer is its solution capacity toward the solute. The infinite dilution capacity toward B is determined by

$$C_B^{\infty} = \frac{1}{\gamma_B^{\infty}} \quad (4)$$

It is worth noting that both the selectivity and capacity are important solvent properties for the economic efficiency of a solvent-based separation process. There is however a trade-off between selectivity and capacity, where increase in the former usually leads to a decrease in the latter.³⁶ Therefore, a simultaneous consideration of these two properties is very important when selecting solvents.

CAMD-based solvent design

Typically, given a set of molecular building groups and objective properties, the CAMD method finds all the different combinations of groups satisfying both molecular structural constraints and property specifications.^{37,38} The successful application of CAMD for solvent design relies on the accurate prediction of solvent physical and thermodynamic properties. The physical properties, such as viscosity and boiling point, can be estimated by simple group contribution (GC) models.³⁹ The thermodynamic properties are usually predicted by GC-based thermodynamic models, such as UNIFAC⁴⁰⁻⁴² and SAFT- γ Mie⁴³.

The molecular design space is fully defined by the selected building groups. Previously, a limited number of groups were considered for solvent design,^{44,45} primarily due to the lack of group-specific thermodynamic parameters. The UNIFAC (Dortmund) consortium interaction parameter matrix (delivery 2016) contains 6506 parameters for 1730 group pairs. This large number of available group interaction parameters makes it possible to design solvents within a large molecular space. This work employs the modified UNIFAC (Dortmund) model⁴⁶ and considers a large number of building blocks consisting of 50 functional groups and 21 single-group molecules (see Table S1 in the Supporting Information).

Owing to the discrete group decisions, the solvent design problems are composed as mixed-integer nonlinear multi-objective optimization problems. In the present work, the solvent selectivity and capacity are maximized subject to solvent structural and property constraints. A detailed mathematical formulation of the problem is given below.

$$\max_{n_j(j=1, 2, \dots, N)} \{S_{AB}^{\infty}, C_B^{\infty}\}$$

Subject to:

(1) Structure and performance relationships

As previously mentioned, two objective functions determined by the following are used.

$$S_{AB}^{\infty} = \gamma_A^{\infty} / \gamma_B^{\infty} \quad (5)$$

$$C_B^{\infty} = 1 / \gamma_B^{\infty} \quad (6)$$

The infinite dilution activity coefficients of n-hexane (A) γ_A^{∞} and methanol (B) γ_B^{∞} are predicted using the reformulated UNIFAC (Dortmund) model approximated with a mixture of $x_A = 0.01$; $x_S = 0.99$ and $x_B = 0.01$; $x_S = 0.99$ at a temperature of 325 K. The activity coefficient of component i in a mixture is determined by the following equations, where i and ii represent component indexes.

$$\ln(\gamma_i) = \ln(\gamma_i^C) + \ln(\gamma_i^R) \quad (7)$$

The UNIFAC theory considers two contributions to the activity coefficient: a combinatorial part (γ_i^C) and a residual part (γ_i^R).

$$\begin{aligned} \ln(\gamma_i^C) = & 0.75 \ln(R_i) - \ln\left(\sum_{ii} x_{ii} R_{ii}^{0.75}\right) - 5Q_i \ln(R_i) - 5Q_i \ln\left(\sum_{ii} x_{ii} Q_{ii}\right) \\ & + 5Q_i \ln(Q_i) + 5Q_i \ln\left(\sum_{ii} x_{ii} R_{ii}\right) - 5Q_i + 1 + C_i \end{aligned} \quad (8)$$

$$C_i = 5 \sum_{ii} x_{ii} Q_{ii} \frac{R_i}{\sum_{ii} x_{ii} R_{ii}} - \frac{R_i^{0.75}}{\sum_{ii} x_{ii} R_{ii}^{0.75}} \quad (9)$$

$$\ln(\gamma_i^R) = R1_i - R2_i \quad (10)$$

$$R1_i = Q_i - \sum_j n_{i,j} q_j \ln(R3_j) + Q_i \ln\left(\sum_{ii} x_{ii} Q_{ii}\right) - \sum_j \frac{R4_{i,j}}{R3_j} \quad (11)$$

$$R2_i = Q_i \ln(Q_i) - \sum_j n_{i,j} q_j \ln\left(\sum_{mj} q_{mj} n_{i,mj} \psi_{mj,j}\right) \quad (12)$$

$$R3_j = \sum_{mj} q_{mj} \sum_{ii} n_{ii,mj} x_{ii} \psi_{mj,j} \quad (13)$$

$$R4_{i,j} = \sum_{mj} n_{i,mj} q_{mj} q_j \sum_{ii} n_{ii,j} x_{ii} \psi_{mj,j} \quad (14)$$

C_i , $R1_i$, $R2_i$, $R3_j$, and $R4_{i,j}$ are intermediate variables.

The van der Waals volume R_i and surface area Q_i for component i are:

$$R_i = \sum_j n_{i,j} r_j \quad (15)$$

$$Q_i = \sum_j n_{i,j} q_j \quad (16)$$

where r_j and q_j are the specific group volume and surface area, respectively.

The group interaction parameters are found in the following equation.

$$\psi_{mj,j} = \exp\left(-\frac{a_{mj,j} + b_{mj,j}T + c_{mj,j}T^2}{T}\right) \quad (17)$$

Here, $a_{mj,j}$, $b_{mj,j}$ and $c_{mj,j}$ are pairwise group-dependent parameters and $n_{i,j}$ is the number of groups j in component i . In the current case study, three components are considered: n-hexane, methanol and the unknown solvent. Thus, $n_{A,j}$ and $n_{B,j}$ are known for hexane and methanol molecules. This leaves $n_{S,j}$ as the decision variable to be optimized, which represents the number of groups j

comprising the solvent molecule. Notably, all equations and expressions used in this work, excluding those contained within the UNIFAC model, only consider the number of groups present in the solvent molecule. This allows us to simplify the notation by omitting the subscript S in $n_{S,j}$ for those equations not pertaining to UNIFAC.

(2) Molecular structural constraints

When optimizing the structure of a solvent molecule by means of a group contribution method, certain structural constraints are required to ensure that the molecular structure of the solvent is physically feasible. These typically include structural feasibility rules as well as constraints to limit the complexity of the molecule.

a) Structural feasibility

One of the common feasibility limitations pertains to the cyclical nature of the molecule. The decision as to which type is considered is determined by three binary variables: y_1 for acyclic, y_2 for bicyclic, and y_3 for monocyclic. Since no two general structures may occur concurrently, these binary variables must sum to one.

$$y_1 + y_2 + y_3 = 1 \quad (18)$$

This is rearranged with the introduction of a new variable m to directly indicate the type of molecule.

$$m - (y_1 - y_2) = 0 \quad (19)$$

where $m = \{-1, 0, 1\}$ represent bicyclic, monocyclic, and acyclic molecules, respectively.

The octet rule (eq. 20) and the modified bonding rule (eq. 21) have to be satisfied. The former ensures that the molecule has no groups with unmatched bonds (i.e., zero valency) and the latter

prevents two neighboring groups from being linked by more than one bond.³⁸ j , m_j and k are group indexes. v_j represents the valency of group j .

$$\sum_{j=1}^N (2 - v_j) n_j - 2m = 0 \quad (20)$$

$$n_j (v_j - 1) + 2 \left(m - \sum_{mj \in \text{Sg}} n_{mj} \right) - \sum_{k=1}^N n_k \leq 0 \quad (\forall j = 1, 2, \dots, N) \quad (21)$$

In total, 71 building blocks consisting of 50 functional groups and 21 single-group molecules are considered (thus N equals 71). The blocks are tabulated in Table S1 together with their IDs, valences, and maximum number of allowed appearances in the molecule. The building groups are further classified into several subset groups. The abbreviated name of each subset and the corresponding ID numbers of the included groups are given in Table 1.

The following constraint prevents more than one single-group solvent from being generated.

$$\sum_{j \in \text{Sg}} n_j \leq 1 \quad (22)$$

If the optimal solvent is found to be a single-group molecule, no other groups are allowed to be added, and the following constraint accounts for this:

$$\sum_{j=1}^N n_j - \sum_{mj \in \text{Sg}} n_{mj} \leq \left(1 - \sum_{mj \in \text{Sg}} n_{mj} \right) n_{max} \quad (23)$$

where n_{max} is the maximum number of groups allowed in the solvent molecule.

Additionally, in the case of aromatics, the total number of aromatic groups (Ag) must equal 6 if the molecule is monocyclic or 10 if it is bicyclic.

$$\sum_{j \in \text{Ag}} n_j = 6y_3 + 10y_2 \quad (24)$$

Eq. 25 – 27 are indispensable for distinguishing among the 3 different hydroxyl groups included in the modified UNIFAC model.

$$n_{\text{CH}_2} - n_{\text{OH}(\text{p})} \geq 0 \quad (25)$$

$$n_{\text{CH}} - n_{\text{OH}(\text{s})} \geq 0 \quad (26)$$

$$n_{\text{C}} - n_{\text{OH}(\text{t})} \geq 0 \quad (27)$$

A constraint is included to ensure that the total number of functional groups is no greater than the total number of main groups.

$$\sum_{j \in (\text{Nceg} \cup \text{Cceg}) \setminus \text{Dtbg}} n_j \leq \sum_{j \in \text{Mg}} n_j \quad (28)$$

b) Structural complexity

In addition to the structural feasibility constraints, structural complexity limitations are also essential for CAMD. The first of these takes the size of typical solvent molecules into account. This is done by limiting the total number of groups involved in creating a molecule using Eq. 29 where n_{\min} is 1 and n_{\max} is set to 6. Additionally, the maximum number allowed for each specific group, $n^{\text{upp}}(j)$, is defined (see Table S1).

$$n_{\min} \leq \sum_{j=1}^N n_j \leq n_{\max} \quad (29)$$

$$0 \leq \text{integer } n_j \leq n_j^{\text{upp}}, (j = 1, 2, \dots, N) \quad (30)$$

The total number of main groups and functional groups is also limited.

$$\sum_{j \in \text{Mg}} n_j \leq 2y_3 + n_{\max}y_1 \quad (31)$$

$$\sum_{j \in (Ceg \cup Nceg \cup Sg) \setminus Dtbg} \frac{n_j}{n_j^{upp}} \leq y_1 + y_3 \quad (32)$$

In aromatic molecules, the groups ACCH, AC, and ACCH₂ exist if the binary variables y_4 , y_5 , and y_6 take the value of one, respectively. y_7 , another binary variable, takes 1 only when both y_5 and y_3 are 1.

$$n_{ACCH}/100 \leq y_4 \leq n_{ACCH} \quad (33)$$

$$n_{AC}/100 \leq y_5 \leq n_{AC} \quad (34)$$

$$n_{ACCH_2}/100 \leq y_6 \leq n_{ACCH_2} \quad (35)$$

$$100 y_7 \geq y_3 + y_5 - 1 \quad (36)$$

$$100 (y_7 - 1) - y_3 - y_5 + 2 \leq 0 \quad (37)$$

The AC group is only allowed to appear at most once in monocyclic molecules and must appear twice in bicyclic molecules.

$$2y_2 + y_7 - n_{AC} = 0 \quad (38)$$

Molecular complexity is further abated by only allowing a maximum of one AC, ACCH or ACCH₂ group to be included in monocyclic molecules.

$$y_4 + y_6 + y_7 \leq 1 \quad (39)$$

Since the ACCH group has two non-aromatic bonds, one of them is restricted to $-\text{CH}_3$ to prevent the generation of too complex molecules.

$$y_4 \leq n_{\text{CH}_3} \quad (40)$$

Additional actions taken to reduce molecular complexity include placing limits on the total number of functional groups (chain-ending and non-chain-ending). Since double and triple bond

containing groups are rarely found in entrainer molecules, the allowed number for these groups is zero.

$$\sum_{j \in C_{eg}} n_j \leq 3y_1 + y_4 + y_6 + y_7 \quad (41)$$

$$\sum_{j \in N_{ceg}} n_j \leq 3y_1 + y_6 + y_7 \quad (42)$$

$$\sum_{j \in D_{ibg}} n_j = 0 \quad (43)$$

(3) Property constraints

In addition to structural constraints, important physical properties that can be predicted by group contribution methods have to be limited as well. One essential characteristic is the melting point of the solvent. The temperature constraint (eq. 44) is used to guarantee that the designed molecules are liquid at room temperature. In order to facilitate the solvent recovery by distillation, a lower bound is placed on the normal boiling point of the solvent (eq. 45).

$$\sum_{j=1}^N n_j t_{m,j} \leq \exp\left(\frac{T_m^{upp}}{T_{m0}}\right) \quad (44)$$

$$\sum_{j=1}^N n_j t_{b,j} \geq \exp\left(\frac{T_b^{low}}{T_{b0}}\right) \quad (45)$$

where $T_m^{upp} = 315$ K, $T_b^{low} = 363$ K, the constants T_{m0} is 147.45 K and T_{b0} is 222.54 K. Group contributions $t_{m,j}$ and $t_{b,j}$ can be found from Marrero and Gani³⁹.

The above multiobjective optimization based CAMD problem is solved using the solution method introduced by Burger et al.⁴³ After solving the optimization problem, we obtain a set of Pareto-optimal solutions, namely butane-1,4-diamine, DMSO, 1,2-ethanediol, 1,4-butanediol,

glycerol, and water. As depicted in Figure 1, butane-1,4-diamine shows the highest solution capacity towards methanol and the lowest separation selectivity. In contrast, water possesses an extremely high selectivity, however, a very low capacity. The tradeoff between these two performance indexes is well captured by three aliphatic alcohols, i.e., 1,2-ethanediol, 1,4-butanediol, and glycerol. Considering the extremely low selectivity of butane-1,4-diamine and the possible reaction with methanol, we only take into account the other five entrainers in the subsequent steps.

RCM analysis

The calculation of residue curve maps (RCMs) is based on the simulation of a batch distillation process where the liquid mixture in a vessel is vaporized and the formed vapor phase is removed continuously.⁴⁷ In this process, the liquid composition changes continually with time. The trajectory of liquid-phase composition is known as a *residue curve* and the RCM is the collection of all such curves for a given system. According to Doherty and Malone⁴⁷, the analysis of RCMs enables the assessment of the suitability of a solvent to promote a mixture separation by extractive distillation.

The simple distillation process is governed by a set of differential equations.

$$\frac{dx}{d\xi} = x - y \quad (46)$$

x represents the liquid-phase mole fraction vector. y denotes the analogous equilibrium vapor-phase mole fractions. ξ is the warped time, a nonlinear transformation of the real time. The RCM can be obtained by integrating eq 46 where the φ - γ method is used to represent the vapor-liquid

equilibrium condition. In this work, the vapor fugacity coefficient φ is 1 due to the ideal gas assumption and the liquid activity coefficient γ is predicted by the modified UNIFAC (Dortmund) model.

We have determined the RCMs for the n-hexane/methanol/solvent systems. The RCM with water as the solvent is shown in Figure 2. As demonstrated, there are two binary azeotropes, one azeotrope between n-hexane and methanol and the other formed between n-hexane and water. These two azeotropic points divide the whole composition map into two distinct regions. In this case, it is not possible to obtain all the pure components by distillation. Therefore, water is not a suitable entrainer for separating n-hexane and methanol by extractive distillation. Due to the fact that the RCMs are very similar for the other four systems, we only show the one with 1,4-butanediol as the solvent in Figure 3. In this RCM, all the residue curves originate from the azeotrope between n-hexane and methanol and terminate at the pure solvent. Only one distillation region can be identified on the map. Therefore, it is possible to obtain all the components as pure products by distillation.

Based on the RCM prediction and analysis, four solvents, namely DMSO ($T_b = 189\text{ }^\circ\text{C}$), 1,2-ethanediol ($197\text{ }^\circ\text{C}$), 1,4-butanediol ($230\text{ }^\circ\text{C}$), and glycerol ($290\text{ }^\circ\text{C}$), are retained as high-potential entrainers for the n-hexane and methanol separation. They will be more rigorously evaluated through the optimal design and analysis of the extractive distillation process.

Extractive distillation process design

An extractive distillation process is fundamentally comprised of an extractive column and a regeneration column. According to the classical setup, the entrainer is normally fed to the

extractive column at the top. The light component, in this work n-hexane, is withdrawn from the distillate, while the heavy component methanol and the entrainer form the bottoms. The entrainer is subsequently separated from methanol in the regeneration column and recycled back to the extractive column. Please note that n-hexane (68 °C) has a higher normal boiling point than methanol (64.7 °C). However, it becomes the light component because the entrainer molecules combine much more closely with methanol.

In this case study, the flow rates of methanol and n-hexane in the feed stream are both set to 500 kmol/h and both the extractive and regeneration columns are operated at atmospheric pressure. For reducing the complexity, the two columns are designed sequentially. Aspen Plus V8.8 is used as the process simulation platform. The entrainer is fed into the top of the extractive column. Based on a preliminary simulation study on the extractive column (1st column) with the four entrainers, it is found that the best feeding location for the hexane/methanol mixture is at about $0.85 \times N_{\text{tot}}^1$ (N_{tot}^1 denotes the total number of stages in this column) and the optimal reflux ratio of the column R_1 is around 0.01. Under these fixed conditions, N_{tot}^1 and the solvent-to-feed molar ratio (S/F) are optimized for each entrainer to minimize the reboiler heat duty (Q_R^1), with a constraint of achieving a 0.995 molar purity of hexane in the distillate stream, x_{Hexane}^{1D} . The solvent regeneration column (i.e., 2nd column) has been optimally designed in a similar way where the total number of stages N_{tot}^2 and reflux ratio R_2 of the column are the key design variables. The objective is to minimize the reboiler heat duty (Q_R^2). The molar purity of the solvent in the bottom product x_{solvent}^{2B} is specified to be no less than 0.9999. The feed is located in the middle of the column.

Figure 4 shows the influence of N_{tot}^1 and S/F on x_{Hexane}^{1D} and Q_R^1 of the extractive column based on different entrainers. Note that it is impossible to satisfy the x_{Hexane}^{1D} purity requirement using

DMSO as the solvent. Therefore, it is not considered as an effective solvent for the investigated separation system. For all the other solvents, i.e., 1,2-ethanediol, 1,4-butanediol, and glycerol, a very similar phenomenon can be observed. As shown in Figure 4, for satisfying the purity specification, the required amount of solvent decreases with the increasing number of stages. To increase the solvent flow rate generally results in a higher reboiler duty (Q_R^1) and the increasing of N_{tot}^1 leads to a larger capital investment. Considering the above facts, we can identify reasonable values for both S/F and N_{tot}^1 . After finding the operation conditions for the extractive column, the design variables for the regeneration column (N_{tot}^2 and R_2) can be optimally selected in a similar way based on the sensitivity study shown in Figure 5.

The operation conditions of the extractive and regeneration columns are indicated by the white circles shown in Figure 4 and Figure 5, respectively. Table 2 summarizes the operating conditions and reboiler heat duties of the extractive distillation process based on different entrainers. As shown, arising from the much higher boiling temperature and enthalpy of vaporization, the glycerol-based process has a substantially higher energy consumption ($Q_R^1 + Q_R^2$) than those of the other two processes. The 1,4-butanediol process shows a slightly lower heat duty than the 1,2-ethanediol process. Besides, the 1,4-butanediol process is expected to consume a smaller capital investment due to its less solvent usage and distillation stages. In view of the above observations, 1,4-butanediol is considered as the best solvent for the n-hexane and methanol separation. Figure 6 illustrates the optimal flowsheet of the extractive distillation process using 1,4-butanediol as the entrainer.

Conclusion

This paper proposes a systematic framework for the optimal design of entrainers for extractive distillation processes. A multi-objective optimization based CAMD method is developed and used to find a set of promising entrainers, which are further screened via rigorous thermodynamic analysis. The extractive distillation process is optimally designed for each of the remaining solvents and the best candidate showing the highest process performance is finally identified. The whole design framework has been illustrated on a selected example of the n-hexane and methanol separation. 1,4-Butanediol is found to be the best entrainer for this separation.

In extractive distillation, it would be wise to also consider several implicit solvent properties such as cost, safety, and toxicity. However, these properties have not been explicitly considered in our CAMD formulation. The reason is that the currently available GC models for predicting the toxicity and environmental impact of solvents cover only a small number of structural groups. There is even no model to estimate the availability and price of solvents. Based on these considerations, we suggest these criteria to be checked individually for the high-potential solvents generated by CAMD.

This work restricts the entrainers to only organic solvents. However, ionic liquids (ILs), a new type of solvent, have received much attention and many novel applications have been developed. Due to their unique and benign properties, ILs as extractive distillation entrainers may offer a series of advantages.⁴⁸ Since the proposed method is not restricted to certain solvent types, such as the conventional organic solvents considered here, it can be easily extended for IL design provided that the thermodynamic parameters between the solutes and IL groups are available.

References

1. Lei, Z.; Li, C.; Chen, B. Extractive distillation: a review. *Sep. Purif. Rev.* **2003**, *32* (2), 121-213.
2. Laroche, L.; Bekiaris, N.; Andersen, H. W.; Morari, M. The curious behavior of homogeneous azeotropic distillation-implications for entrainer selection. *AIChE J.* **1992**, *38* (9), 1309-1328.
3. Ivonne, R. D.; Vincent, G.; Xavier, J. Heterogeneous entrainer selection for the separation of azeotropic and close boiling temperature mixtures by heterogeneous batch distillation. *Ind. Eng. Chem. Res.* **2001**, *40* (22), 4935-4950.
4. Gani, R.; Brignole, E. A. Molecular design of solvents for liquid extraction based on UNIFAC. *Fluid Phase Equilibr.* **1983**, *13*, 331-340.
5. Gani, R.; Jiménez-González, C.; Constable, D. J. Method for selection of solvents for promotion of organic reactions. *Comput. Chem. Eng.* **2005**, *29*, 1661-1676.
6. Stanescu, I.; Achenie, L. E. A theoretical study of solvent effects on Kolbe–Schmitt reaction kinetics. *Chem. Eng. Sci.* **2006**, *61*, 6199-6212.
7. Folić, M.; Adjiman, C. S.; Pistikopoulos, E. N. Design of solvents for optimal reaction rate constants. *AIChE J.* **2007**, *53*, 1240-1256.
8. Folić, M.; Adjiman, C. S.; Pistikopoulos, E. N. Computer-aided solvent design for reactions: maximizing product formation. *Ind. Eng. Chem. Res.* **2008**, *47*, 5190-5202.
9. Struebing, H.; Ganase, Z.; Karamertzanis, P. G.; Sioukrou, E.; Haycock, P.; Piccione, P. M.; Armstrong, A.; Galindo, A.; Adjiman, C. S. Computer-aided molecular design of solvents for accelerated reaction kinetics. *Nat. Chem.* **2013**, *5*, 952-957.
10. Zhou, T.; McBride, K.; Zhang, X.; Qi, Z.; Sundmacher, K. Integrated solvent and process design exemplified for a Diels-Alder reaction. *AIChE J.* **2015**, *61*, 147-158.
11. Zhou, T.; Lyu, Z.; Qi, Z.; Sundmacher, K. Robust design of optimal solvents for chemical reactions — A combined experimental and computational strategy. *Chem. Eng. Sci.* **2015**, *137*, 613-625.
12. Zhou, T.; Wang, J.; McBride, K.; Sundmacher, K. Optimal design of solvents for extractive

reaction processes. *AIChE J.* **2016**, *62*, 3238-3249.

13. Austin, N. D.; Sahinidis, N. V.; Konstantinov, I. A.; Trahan, D. W. COSMO-based computer-aided molecular/mixture design: A focus on reaction solvents. *AIChE J.* **2018**, *64* (1), 104-122.
14. Marcoulaki, E. C.; Kokossis, A. C. On the development of novel chemicals using a systematic optimisation approach. Part II. Solvent design. *Chem. Eng. Sci.* **2000**, *55*, 2547-2561.
15. Kim, K. J.; Diwekar, U. M. Integrated solvent selection and recycling for continuous processes. *Ind. Eng. Chem. Res.* **2002**, *41*, 4479-4488.
16. Karunanithi, A. T.; Achenie, L. E. K.; Gani, R. A new decomposition-based computer-aided molecular/mixture design methodology for the design of optimal solvents and solvent mixtures. *Ind. Eng. Chem. Res.* **2005**, *44*, 4785-4797.
17. Karunanithi, A. T.; Achenie, L. E. K.; Gani, R. A computer-aided molecular design framework for crystallization solvent design. *Chem. Eng. Sci.* **2006**, *61*, 1247-1260.
18. McLeese, S. E.; Eslick, J. C.; Hoffmann, N. J.; Scurto, A. M.; Camarda, K. V. Design of ionic liquids via computational molecular design. *Comput. Chem. Eng.* **2010**, *34*, 1476-1480.
19. Roughton, B. C.; Christian, B.; White, J.; Camarda, K. V.; Gani, R. Simultaneous design of ionic liquid entrainers and energy efficient azeotropic separation processes. *Comput. Chem. Eng.* **2012**, *42*, 248-262.
20. Chávez-Islas, L. M.; Vasquez-Medrano, R.; Flores-Tlacuahuac, A. Optimal molecular design of ionic liquids for high-purity bioethanol production. *Ind. Eng. Chem. Res.* **2011**, *50* (9), 5153-5168.
21. Valencia-Marquez, D.; Flores-Tlacuahuac, A.; Vasquez-Medrano, R. Simultaneous optimal design of an extractive column and ionic liquid for the separation of bioethanol-water mixtures. *Ind. Eng. Chem. Res.* **2011**, *51* (17), 5866-5880.
22. Samudra, A. P.; Sahinidis, N. V. Optimization-based framework for computer-aided molecular design. *AIChE J.* **2013**, *59*, 3686-3701.
23. Austin, N. D.; Sahinidis, N. V.; Trahan, D. W. A COSMO-based approach to computer-aided mixture design. *Chem. Eng. Sci.* **2017**, *159*, 93-105.

24. Zhang, J.; Qin, L.; Peng, D.; Zhou, T.; Cheng, H.; Chen, L.; Qi, Z. COSMO-descriptor based computer-aided ionic liquid design for separation processes: Part II: Task-specific design for extraction processes. *Chem. Eng. Sci.* **2017**, *162*, 364-374.
25. Lek-utaiwan, P.; Suphanit, B.; Douglas, P. L.; Mongkolsiri, N. Design of extractive distillation for the separation of close-boiling mixtures: Solvent selection and column optimization. *Comput. Chem. Eng.* **2011**, *35* (6), 1088-1100.
26. Jensen, N.; Coll, N.; Gani, R. An integrated computer aided system for generation and evaluation of sustainable process alternatives. *Technological Choices for Sustainability* **2004**, 183-214.
27. Kossack, S.; Kraemer, K.; Gani, R.; Marquardt, W. A systematic synthesis framework for extractive distillation processes. *Chem. Eng. Res. Des.* **2008**, *86* (7), 781-792.
28. Chen, B.; Lei, Z.; Li, Q.; Li, C. Application of CAMD in separating hydrocarbons by extractive distillation. *AIChE J.* **2005**, *51* (12), 3114-3121.
29. Lei, Z.; Arlt, W.; Wasserscheid, P. Separation of 1-hexene and n-hexane with ionic liquids. *Fluid Phase Equilibr.* **2006**, *241* (1-2), 290-299.
30. Eden, M. R.; Jorgensen, S. B.; Gani, R.; El-Halwagi, M. M. A novel framework for simultaneous separation process and product design. *Chem. Eng. Process.* **2004**, *43*, 595-608.
31. Eljack, F. T.; Eden, M. R.; Kazantzi, V.; Qin, X.; El-Halwagi, M. M. Simultaneous process and molecular design – A property based approach. *AIChE J.* **2007**, *53*, 1232-1239.
32. Papadopoulos, A. I.; Linke, P. Multiobjective molecular design for integrated process-solvent systems synthesis. *AIChE J.* **2005**, *52*, 1057-1070.
33. Papadopoulos, A. I.; Linke, P. Efficient integration of optimal solvent and process design using molecular clustering. *Chem. Eng. Sci.* **2006**, *61*, 6316-6336.
34. Bardow, A.; Steur, K.; Gross, J. Continuous-molecular targeting for integrated solvent and process design. *Ind. Eng. Chem. Res.* **2010**, *49*, 2834-2840.
35. Song, Z.; Zhang, C.; Qi, Z.; Zhou, T.; Sundmacher, K. Computer-aided design of ionic liquids as solvents for extractive desulfurization. *AIChE J.* **2018**, *64* (3), 1013-1025.
36. Krummen, M.; Gruber, D.; Gmehling, J. Measurement of activity coefficients at infinite dilution in solvent mixtures using the dilutor technique. *Ind. Eng. Chem. Res.* **2000**, *39* (6),

2114-2123.

37. Gani, R.; Nielsen, B.; Fredenslund, A. A group contribution approach to computer-aided molecular design. *AIChE J.* **1991**, *37*, 1318-1332.
38. Odele, O.; Macchietto, S. Computer aided molecular design: A novel method for optimal solvent selection. *Fluid Phase Equilibr.* **1993**, *82*, 47-54.
39. Marrero, J.; Gani, R. Group-contribution based estimation of pure component properties. *Fluid Phase Equilibr.* **2001**, *183*, 183-208.
40. van Dyk, B.; Nieuwoudt, I. Design of solvents for extractive distillation. *Ind. Eng. Chem. Res.* **2000**, *39*, 1423-1429.
41. Cheng, H. C.; Wang, F. S. Trade-off optimal design of a biocompatible solvent for an extractive fermentation process. *Chem. Eng. Sci.* **2007**, *62*, 4316-4324.
42. Zhou, T.; Zhou, Y.; Sundmacher, K. A hybrid stochastic–deterministic optimization approach for integrated solvent and process design. *Chem. Eng. Sci.* **2017**, *159*, 207-216.
43. Burger, J.; Papaioannou, V.; Gopinath, S.; Jackson, G.; Galindo, A.; Adjiman, C. S. A hierarchical method to integrated solvent and process design of physical CO₂ absorption using the SAFT- γ Mie approach. *AIChE J.* **2015**, *61* (10), 3249-3269.
44. Wang, Y.; Achenie, L. E. K. Computer aided solvent design for extractive fermentation. *Fluid Phase Equilibr.* **2002**, *201*, 1-18.
45. Gebreslassie, B. H.; Diwekar, U. M. Efficient ant colony optimization for computer aided molecular design: case study solvent selection problem. *Comput. Chem. Eng.* **2015**, *78*, 1-9.
46. Jakob, A.; Grensemann, H.; Lohmann, J.; Gmehling, J. Further development of modified UNIFAC (Dortmund): Revision and extension 5. *Ind. Eng. Chem. Res.* **2006**, *45* (23), 7924-7933.
47. Doherty, M. F.; Malone, M. F. *Conceptual Design of Distillation Systems*; McGraw-Hill: New York, 2001.
48. Lei, Z.; Dai, C.; Zhu, J.; Chen, B. Extractive distillation with ionic liquids: a review. *AIChE J.* **2014**, *60* (9), 3312-3329.

Table 1: Group classes, ID numbers, and abbreviated names of the subset groups

Group class	Group ID number	Abbreviation
Main groups	1-4	Mg
Double and triple bond groups	5-9	Dtbg
Aromatic groups	10-14, 18, 31, 38-41, 47	Ag
Non-chain-ending functional groups	6-8, 20, 23, 26, 27, 30, 35, 36, 43, 50	Nceg
Chain-ending functional groups	5, 9, 15-17, 19, 21, 22, 24, 25, 28, 29, 32-34, 37, 42, 44-46, 48, 49	Ceg
Single-group molecules	51-71	Sg

Table 2: The operating conditions and reboiler heat duties of the extractive distillation process
based on different entrainers

Solvent	1,2-Ethandiol	1,4-Butanediol	Glycerol
N_{tot}^1	18	14	10
S/F	1.30	0.78	0.90
Q_R^1 (kW)	9473.5	9548.6	8328.8
N_{tot}^2	8	9	17
R_2	0.085	0.038	0.150
Q_R^2 (kW)	11698.4	11549.8	18519.5
$Q_R^1 + Q_R^2$ (kW)	21171.9	21098.4	26848.3

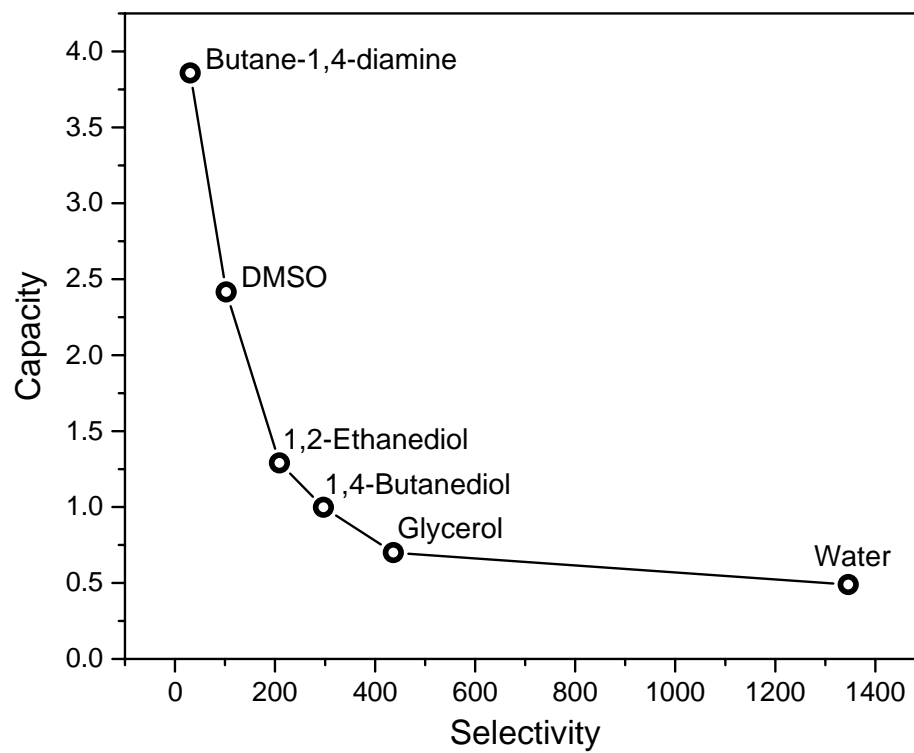


Figure 1: Solution of the MOO-CAMD based solvent design problem

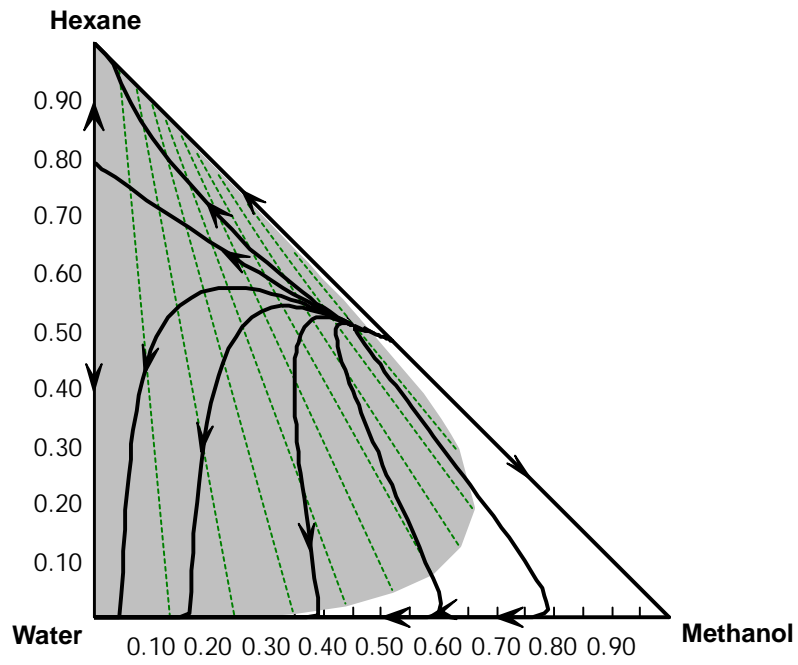


Figure 2: Residue curve map for the n-hexane/methanol/water ternary system

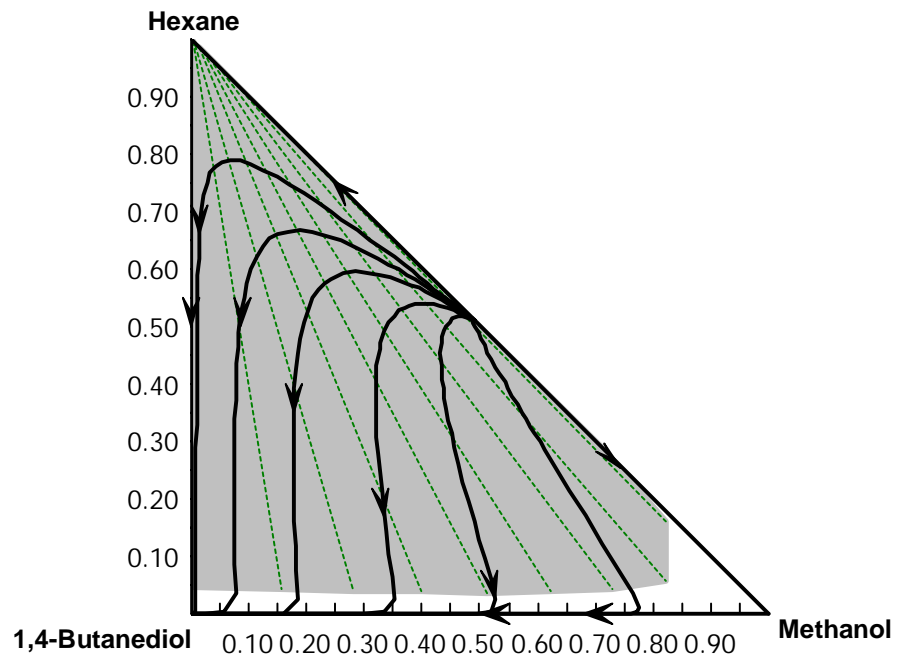


Figure 3: Residue curve map for the n-hexane/methanol/1,4-butanediol ternary system

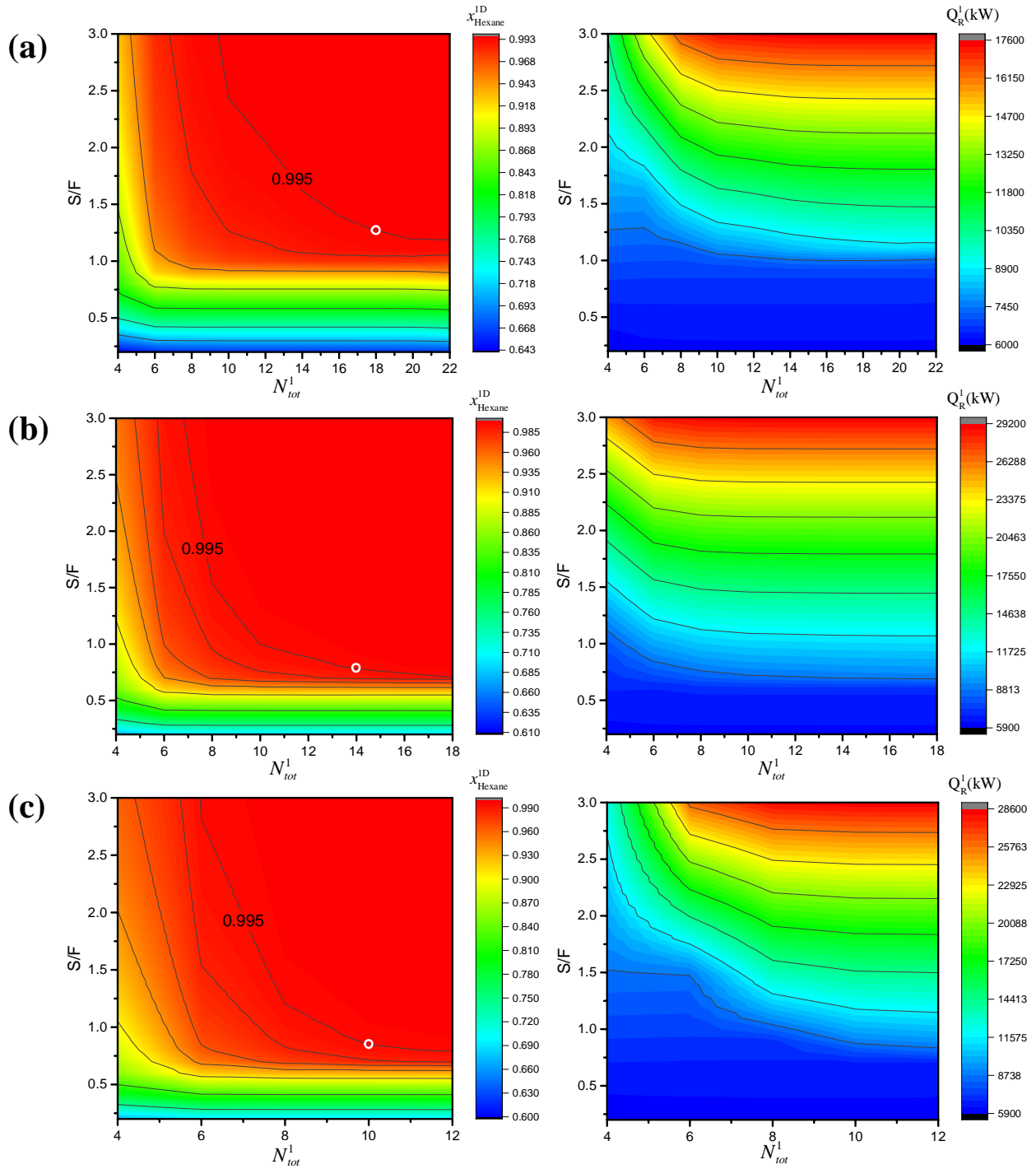


Figure 4: The influence of N_{tot}^1 and S/F on x_{Hexane}^{1D} and Q_R^1 using 1,2-ethanediol (a), 1,4-butanediol (b), and glycerol (c) as the solvent

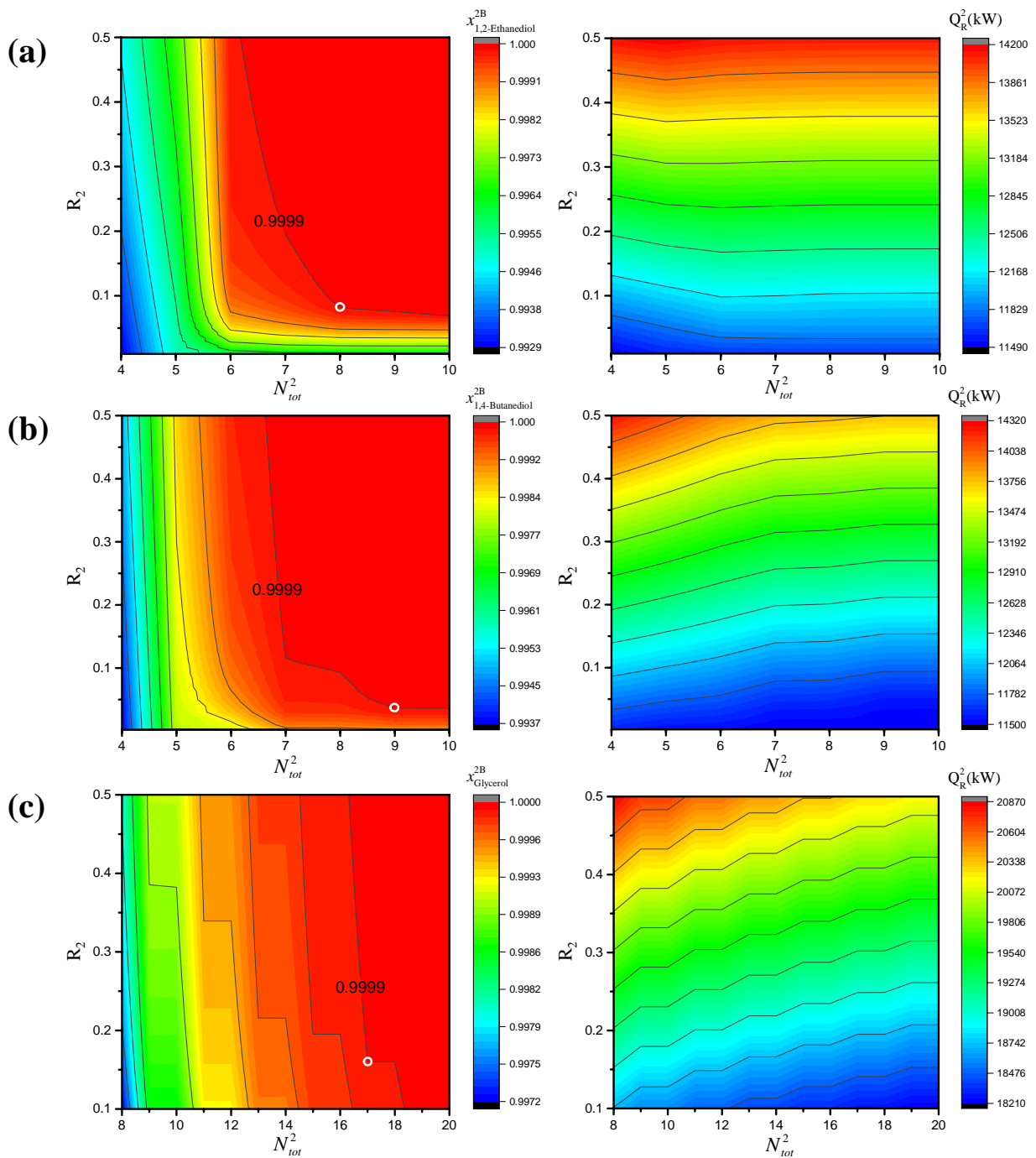


Figure 5: The influence of N_{tot}^2 and R_2 on x_{solvent}^{2B} and Q_R^2 using 1,2-ethanediol (a), 1,4-butanediol (b), and glycerol (c) as the solvent

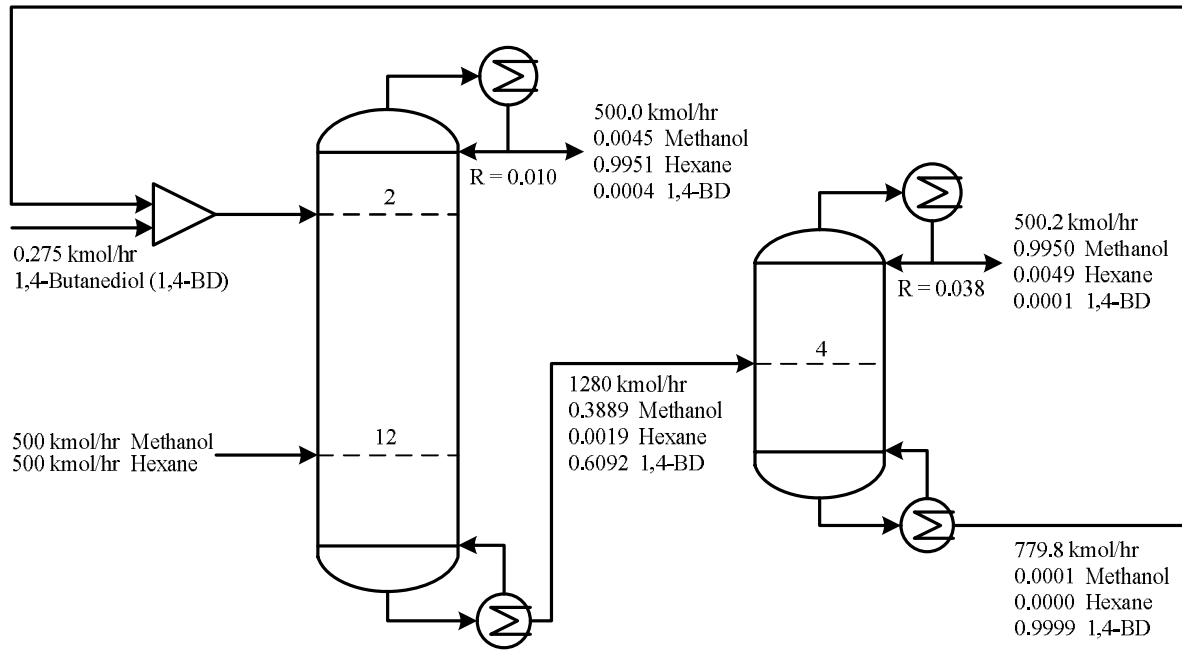












Figure 6: The optimal flowsheet of the extractive distillation process using 1,4-butanediol (1,4-BD) as the solvent

Graphic Abstract

- | | |
|--|---|
|  CH_n (alkyl) |  OH (hydroxyl) |
|  CH_n [in alcohols] |  COOH (carboxyl) |
|  CH_n [in hydrophobic tails of alcohols] |  CH_nCO (ketone) |
|  $\text{CH}_n(\text{OH})$ [with OH-group] |  CH_nO (ether) |
|  C=C (alkenyl) |  CCOO (ester) |

